Predicting ocean rogue waves from point measurements:
An experimental study for unidirectional waves

Will Cousins,[1] Miguel Onorato,[2,3] Amin Chabchoub,[4] and Themistoklis P. Sapsis[1,*]

[1]*Department of Mechanical Engineering, Massachusetts Institute of Technology, Cambridge, Massachusetts 02139, USA*
[2]*Dipartimento di Fisica, Università degli Studi di Torino, 10125 Torino, Italy*
[3]*Istituto Nazionale di Fisica Nucleare, INFN, Sezione di Torino, 10125 Torino, Italy*
[4]*School of Civil Engineering, The University of Sydney, Sydney NSW 2006, Australia*

Rogue waves are strong localizations of the wave field that can develop in different branches of physics and engineering, such as water or electromagnetic waves. Here, we experimentally quantify the prediction potentials of a comprehensive rogue-wave reduced-order precursor tool that has been recently developed to predict extreme events due to spatially localized modulation instability. The laboratory tests have been conducted in two different water wave facilities and they involve unidirectional water waves; in both cases we show that the deterministic and spontaneous emergence of extreme events is well predicted through the reported scheme. Due to the interdisciplinary character of the approach, similar studies may be motivated in other nonlinear dispersive media, such as nonlinear optics, plasma, and solids, governed by similar equations, allowing the early stage of extreme wave detection.

I. INTRODUCTION

Rogue waves, also known as freak waves, are abnormally large waves with crest-to-trough height exceeding two times the significant wave height [1–5]. Although rare (approximately three waves per day in a single point measurement, using linear theory, and an average wave period of 10 s), these waves can have dramatic effects on ships and other ocean structures [6,7]. Therefore, predicting such extreme events is an important challenging topic in the field of ocean engineering, as well as other fields of wave physics, including plasma [8], solids [9], and optics [10–12]. In addition, from a mathematical viewpoint the short-term prediction problem of extreme events in nonlinear waves presents particular interest due to the stochastic character of water waves and also the inherent complexity of the governing equations.

Before discussing in detail the emphasized prediction tool for rogue waves, we find it relevant to make a general statement on the predictability of surface gravity waves. In [13] it has been shown numerically that 2D (i.e., in two horizontal dimensions) ocean waves are described by a chaotic system; this implies that due to positive Lyapunov exponents, after some time (space) the system loses memory of the initial condition and any attempt to perform a deterministic forecast will generally fail. Annenkov and Shrira [13] found that a timescale of predictability for typical steepness of ocean waves is of the order of 1000 wave periods. For larger times, predictions, including rogue-wave forecast, can be made only on a statistical basis, i.e., given a wave spectrum and its evolution, the goal is to establish the probability distribution of wave height or wave crest for the given sea state. This allows one to calculate the probability of encountering a wave whose height is larger than a certain threshold (usually 2 times the significant wave height); see, for example, [14]. On shorter timescales, a deterministic prediction of rogue waves is generally possible. In [15] a predictability time scale for rogue waves was estimated through extensive numerical simulations using a phase-resolved high-order spectral technique [16,17]. It was demonstrated that a timescale for reliable prediction can be $\mathcal{O}(10T_p)$, where T_p is the peak period of the spectrum.

For long-crested water waves, statistics are far from Gaussian, with heavy tails [18–21]. In this case, the dominant mechanism for the formation of large waves is finite-time instabilities rising in the form of a spatially localized modulation instability [14,22,23]. For deep water waves, a manifestation of this focusing is the well-known modulation instability of a plane wave to small sideband perturbations [24,25]. This instability, which has been demonstrated experimentally since the 1960s [26,27] and its limiting case more recently [28,29], generates significantly focused coherent structures by soaking up energy from the nearby field [30–32]. In this context it is possible and more advantageous to study the dynamics of wave groups (in contrast to individual waves) through reduced-order representations [23,33,34], alleviating the direct numerical treatment of the full equations. Depending on the typical dimensions (length, width, height) of the wave group, we may have subsequent modulation instability, which leads to further significant magnification of the wave group height. Such critical wave groups can be formed by the random superposition of different harmonics, see Fig. 1. If a wave group has appropriate characteristics, it will amplify due to modulation instability. Such nonlinear evolution can be
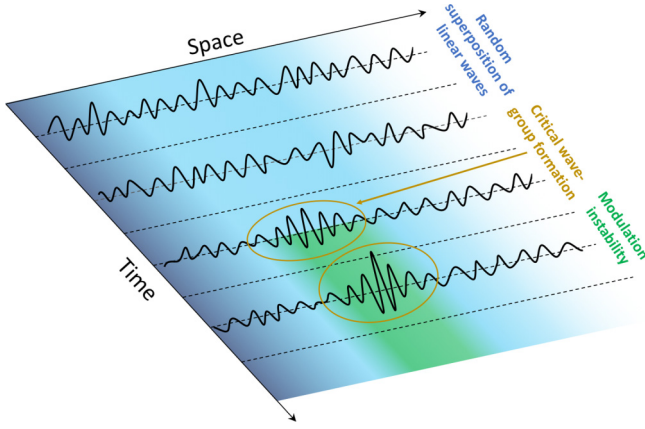
---

*Corresponding author: sapsis@mit.edu

FIG. 1. In the typical regime the dominant mechanism for the wave group formation is the superposition of linear waves. If a critical wave group is formed, i.e., one with sufficiently large length and amplitude, the strongly nonlinear dynamics associated with modulation instability can be foreseen through simple precursors.

foreseen using simple precursors that quantify the conditions for modulation instability of the wave group, as shown in Fig. 1.

A reduced-order precursor for the prediction of rogue waves, caused by spatially localized modulation instability, has been proposed for unidirectional [35,36] as well as directional [37] surface gravity waves. The idea behind it comes from combining spectral information for the sea state and information involving the evolution of isolated wave groups to rogue waves. The derived precursors have the form of characteristic patterns that precede rogue waves $\mathcal{O}(10T_p)$ ahead. Using field information (i.e., wave measurements with spatial extend) for the region of interest, the predictive scheme *quickly* identifies locations where these patterns are present and provides the estimated magnitude of a rogue wave that will occur in the near future, close to this location. The developed scheme is particularly robust, given that it relies on the detection of large-scale features (having the size of the wave group) utilizing either temporal or spatial measurements. For this reason the scheme does not depend on small-scale measurement errors. In addition, it is extremely fast due to the fact that there is no need to calculate any solution of any evolution equation involved in the prediction process. The method of precursors has been validated in numerically generated wave fields described by the modified nonlinear Schrödinger equation [38] for (i) unidirectional waves [36] and (ii) directional waves [37]. In both cases, water waves that follow Gaussian and the JONSWAP spectrum were considered. Note that another approach based on the spectral signatures of wave groups that evolve into rogue waves has been proposed in [39,40]. The basic idea is to look at the spectrum over small, localized windows in order to detect universal triangular signatures associated with the early stages of doubly localized extreme coherent structures.

The primary significance of this work is the application of a data-driven predictive scheme to successfully predict the occurrence of extreme waves in a laboratory setting, caused by spatially localized modulation instability. This scheme is similar to the scheme developed in [35,36]. Our starting point

is the modified nonlinear Schrödinger equation (MNLS) [38], formulated as an evolution equation in space rather than in time [41]. The analysis of this universal equation, that can be also applied to a wide range of physical media (for instance, in optics [42]), allows for the characterization of wave groups or pulses as critical to become either rogue or not through single point measurements of the time series of the surface elevation. We demonstrate the effectiveness of the developed scheme through experimental hydrodynamic data in the form of time series of water wave profiles. Using multiple realizations of rogue waves, we statistically quantify the accuracy of the developed scheme.

The main distinction of the present work is that in prior work the predictive scheme was applied only in the context of forecasting the propagation of a wave field through numerical simulations of the MNLS. It is true that the laboratory experiments considered here are overly simplistic representations of realistic ocean dynamics. However, the work presented here represents a significant step forward in reduced-order forecasting of extreme events, demonstrating that this scheme can provide accurate spatiotemporal predictions in an experimental environment with noisy measurements.

II. PRECURSORS BASED ON POINT MEASUREMENTS

Our goal is to predict extreme waves in unidirectional wave fields on the surface of deep water using time measurements at a single point with satisfactory high sampling frequency. The developed scheme consists of an offline, as well as an online, real-time component. For the offline component, we quantify the critical wave groups that evolve to rogue waves using direct numerical solutions of the MNLS equation. Here we employed the MNLS equation for demonstration purposes; the fully nonlinear water wave equations could also be used, but the offline component would be computationally more expensive. In the online, real-time component, we identify the coherent wave groups in measurements of a physical, irregular wave time-series. We then use the results from the offline component to predict how the measured groups will evolve.

The scheme we discuss here closely follows the ideas presented in [35]. In this case the prediction analysis was based on the availability of field measurements. The algorithm reported in this work predicts future extreme waves from time-series measurements of the wave field at a single point. Such formulation yields a tremendous practical payoff, since it allows for the application of the algorithm to experimental data as well as its potential application to more realistic oceanic setups.

A. Evolution of isolated, localized groups

We begin by performing an analysis of localized wave groups using the space-time version of the MNLS [38]:

$$\frac{\partial u}{\partial x} + \frac{2k}{\omega}\frac{\partial u}{\partial t} + \mathrm{i}\frac{k}{\omega^2}\frac{\partial^2 u}{\partial t^2} + \mathrm{i}k^3|u|^2 u$$
$$- \frac{k^3}{\omega}\left(6|u|^2\frac{\partial u}{\partial t} + 2u\frac{\partial |u|^2}{\partial t} - 2\mathrm{i}u\mathcal{H}\left[\frac{\partial |u|^2}{\partial t}\right]\right) = 0, \quad (1)$$

where u is the envelope of the wave train, ω is the dominant angular frequency, related to the wave number k through the

dispersion relation $\omega^2/g = k$, and $\mathcal{H}$ is the Hilbert transform, defined in Fourier space as

$$\mathcal{F}[\mathcal{H}[f]](\omega) = \mathrm{i}\,\mathrm{sgn}(\omega)\mathcal{F}[f](\omega).$$

The above MNLS equation was derived from the fully nonlinear equations for potential flow on the surface of a deep fluid [41]. The wave field is assumed to be narrow banded and the steepness small. To leading order, the surface elevation $\eta(x,t)$ is given by

$$\eta(x,t) = \Re[u(x,t)\exp{(\mathrm{i}(kx - \omega t))}]; \qquad (2)$$

higher-order corrections may also be included. (See, for instance, Refs. [19,43].)

While the standard form of MNLS (time-space) can be used to understand how *spatially* defined wave groups will evolve in future times [35,36], the above formulation allows us to predict how *temporally* defined wave groups (over a single point) will evolve in space. For this reason it is an appropriate advantageous formulation in the case where we aim to rely on just one point measurement (over time) in order to predict the occurrence of a rogue wave downstream of the wave propagation. We emphasize that the proposed time-domain analysis and prediction can be also applied to electromagnetic waves [44].

To investigate the evolution of localized wave groups due to localized modulation instability, we consider boundary data of the form

$$u(x = 0, t) = A_0 \,\mathrm{sech}(t/\tau_0). \qquad (3)$$

The choice of such function is not related to any special solution of the nonlinear Schrödinger (NLS) equation but rather by the fact that it has the shape of a wave group (a Gaussian shaped function would imply the same type of dynamics). Therefore, we numerically evolve such groups for different amplitudes A_0 and periods τ_0. In fact, for each (A_0, τ_0) pair, in the case of group focusing, we record the value of the amplitude of the group at maximum focus [45]. We emphasise that the parameters here considered are not in the semiclassical regime, i.e., in the small dispersion limit, as considered in [46]. In Fig. 2, we display the group amplification factor as a function of A_0 and τ_0 due to nonlinear (modulation instability) effects. Similar to [23], we can notice that indeed some groups focus and increase in amplitude while others defocus and do not grow. These focusing groups may act as a trigger for the occurrence of extreme waves in unidirectional wave fields, and therefore, we may be able to predict extreme waves in advance by detecting such packets. We mention that a number of the cases pictured would yield breaking waves in a physical setting. Although the equation we consider does not include such effects, the wave breaking threshold is typically taken to be $|u| = 0.4$ [47]; the initial wave group parameters (A_0, L_0) that lead to wave groups that satisfy this threshold limit are marked with a white curve in Fig. 2. A similar figure has been reported in [36] but obtained using the time-space version of the MNLS, while the results presented here refer to wave groups in time evolved using the space-time version of MNLS, which is the appropriate setting for this experimental study. Note that the moment we predict wave breaking the steepness of the wave field is
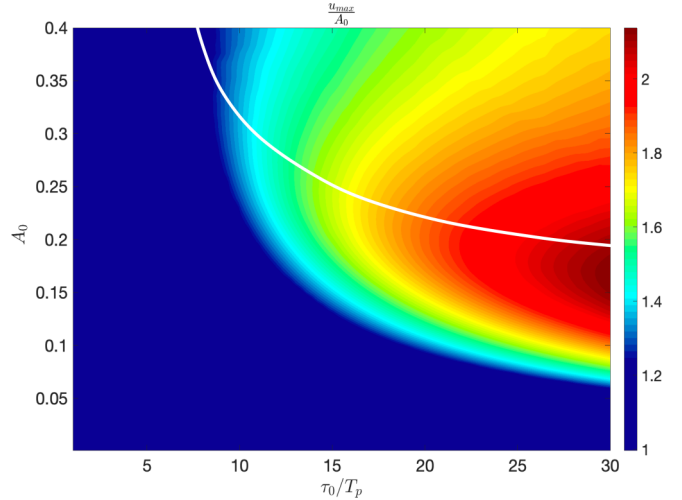

FIG. 2. Amplification factor for group evolution due to localized modulation instability. An amplification factor of 1 indicates that the group defocuses and does not increase in amplitude. The white line indicates which wave groups exceed the wave breaking threshold of $|u| = 0.4$ during their evolution. This figure was generated by evolution simulations of the nondimensionalized MNLS.

generally small and the equations are valid. This may not be the case in a later time instant when wave breaking can occur. However, this does not compromise our prediction capability. We also emphasize that the Peregrine soliton has similar physical features as multisolitons [46], while the choice of carrier parameters allows the observation of the focusing stage of unstable wave packets within the limited length of the water wave flume [28,48,49].

B. Prediction methodology

In the proposed prediction scheme the validation will be based on time-series data describing the evolution of waves in experimental water wave facilities. This data provides several measurements at different stages of wave evolution for the surface elevation η at different single spatial points. To make a future forecast at probe location x^* at time t^* we follow the steps as described below:

(1) Compute the envelope by Hilbert transform and apply a band pass filter in order to remove the higher harmonics, as suggested in [50,51], using measurements of $\eta(x^*, t)$, $t \leqslant t^*$.

(2) Apply a scale selection algorithm, described in [36], to detect coherent wave groups and their amplitude A_0 and wave group period τ_0.

(3) For each group, we estimate the future elevation of the wave field by interpolating the results from the localized wave group numerical experiment, see Fig. 2.

Note that the above procedure can accurately predict the degree of subsequent magnification of the wave group due to localized modulation instability. However, aside from a rough estimate on the time required for the nonlinear growth to occur, it does not provide us with the exact location of the rogue-wave focusing.

III. ANALYSIS OF TWO SETS OF EXPERIMENTAL DATA

Hereafter, we will apply the scheme to two types of experiments performed in different water wave facilities. In the first experimental campaign, the idea is to embed a particular solution of the NLS equation that is known to focus, in an irregular and realistic sea state. For this purpose, we apply to the wave maker a NLS Peregrine-type solution, known to describe nonlinear rogue-wave dynamics. In fact, breathers generally describe the nonlinear stage of modulation instability as well as wave focusing. Being the limiting case with an infinite modulation period, the Peregrine solution is a doubly localized coherent structure that models extreme events on a regular background [52]. As such, its evolution in a chaotic wave field, as well as the detection of its early stage of evolution through a finite window length in such irregular conditions, are not self-evident. In this case the Peregrine-type boundary conditions launched into the wave maker have been modeled to be embedded into a typical ocean JONSWAP spectrum. More details on the construction methodology can be found in [53]. In this study, the goal is to address the problem of whether it would be possible to detect Peregrine-type rogue-wave solutions at the early stages of wave focusing, once embedded in a random sea state.

The second experimental study consists in generating a JONSWAP spectrum with random phases and observing the spontaneous formation of extreme oceanic waves. Here, the reported scheme is applied to the time series closest to the wave maker in order to establish an early stage of extreme wave event forecast, avoiding any computational effort in simulating their evolution, predicting the rogue-wave formation in the water wave facility.

A. Critical wave groups embedded in irregular sea configurations

We recall that breathers are exact solutions of the non-linear Schrödinger equation [3,50]. Some of them describe the nonlinear stage of a classical modulation instability process, namely, of a periodically perturbed wave field [54,55]. The case of an infinite modulation period is known as the Peregrine breather [52] that has been so far observed in three different physical systems: optics, hydrodynamics, and plasma [8,28,56]. The relevance of the Peregrine solution in the rogue-wave context is related to its significant amplitude amplification of 3 and to its double localization in both time and space.

1. Description of experiments

The experimental stability analysis of the Peregrine solution is a substantial scientific issue to tackle if one is connecting this basic simplified model to be relevant to ocean engineering applications. To achieve this, initial conditions for a hydrodynamic experiment have been constructed, embedding a Peregrine solution into JONSWAP sea states. The purpose of this experiment is to demonstrate that our method is robust and is able to capture a rogue for the case where smaller random waves are present. We recall that a unidirectional JONSWAP sea is defined, satisfying the following spectral
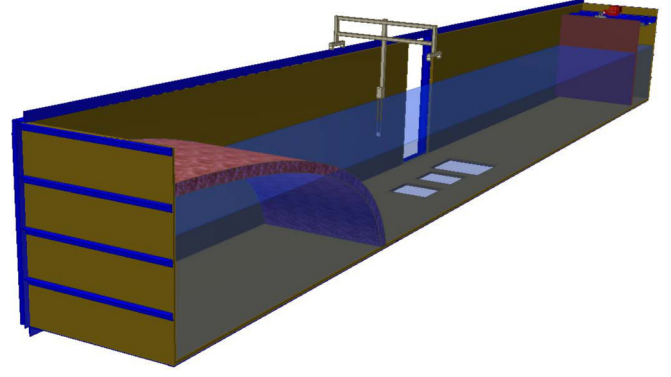

FIG. 3. Water wave facility in which the Peregrine breather has been embedded in a JONSWAP sea state configuration. Its dimensions are $15 \times 1.5 \times 1$ m^3.

distribution [57]:

$$S(f) = \frac{\alpha}{f^5} \exp\left[-\frac{5}{4}\left(\frac{f_p}{f}\right)^4\right]\gamma^{\exp\left[-\frac{(f-f_p)^2}{2\sigma^2 f_p^2}\right]}, \quad (4)$$

where f_p corresponds to the peak frequency of the spectrum, $\sigma = 0.07$ if $f \leqslant f_p$ and $\sigma = 0.09$ if $f > f_p$, α is the so-called Phillips parameter, and γ is the enhancement, or peakedness parameter. Once the peak frequency of the spectrum is fixed, in experiments one usually chooses α and γ to select the significant height (defined as 4 times the square root of the area under the spectrum) and the spectral bandwidth. The surface displacement can be obtained from the spectrum by

$$\eta_{\text{JONSWAP}}(0, t) = \sum_{n=1}^{N} \sqrt{2S(f_n)\Delta f_n} \cos\left(2\pi f_n t - \phi_n\right), \quad (5)$$

with random phases $\phi_n \in [0, 2\pi)$ [58]. Details of the Fourier space construction methodology are described in [53]. In fact, the wave elevation at $x = 0$ (the location of the wave maker) has been constructed to satisfy a JONSWAP sea state configuration with a significant wave height of $H_s = 0.025$ m, as well as a spectral peakedness parameter of $\gamma = 6$. The wave peak frequency f_p is 1.7 Hz; thus the characteristic steepness, defined as $H_s k_p/2$ with $k_p = (2\pi f_p)^2/g$, is 0.15, which is a realistic value for ocean waves [57]. This allows us to track the evolution of an unstable packet in time and space in irregular conditions while evolving, for instance, in a water wave facility rather than assuming spontaneous emergence, as discussed in the next section. The experiments have been conducted in a water wave facility with a flap-type wave maker. Its length is 15 m with a width of 1.5 m, while the water depth is 1 m, as schematically depicted in Fig. 3 and described in [59]. Capacitance wave gauges have been placed along the facility to measure the temporal variation of the water surface elevation.

2. Assessment of the scheme

In the following, we apply the prediction scheme to the wave tank measurements, related to the experiments of an embedded Peregrine model in unidirectional sea state conditions. The wave propagation of both the Peregrine-type dynamics excited as well as an independent spontaneous focusing and
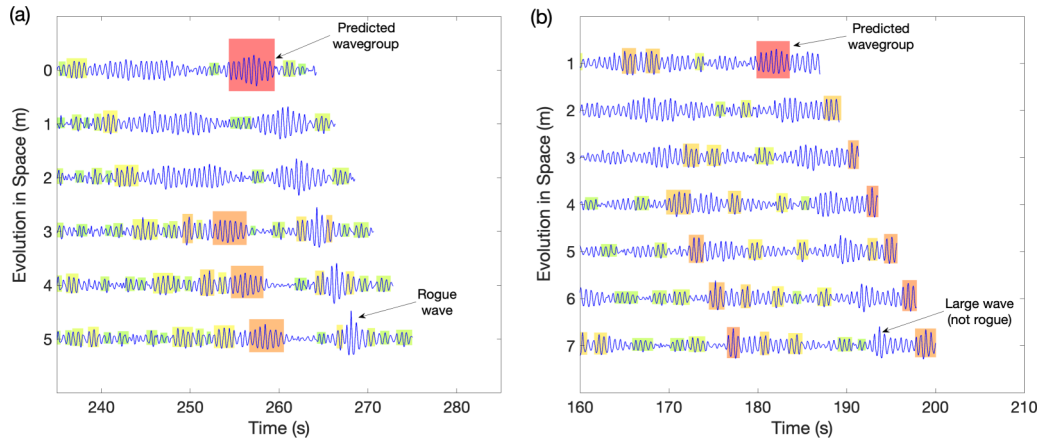
FIG. 4. (a) Successful prediction of a rogue wave occurring through the embedding of a Peregrine soliton into an irregular background for $\gamma = 6$. (b) A false-positive prediction leading to a large wave which does not overpass the rogue-wave threshold (from a different time window of the same experiment displayed on the left). The blue curves indicate the experimental measurements. The colored boxes show the prediction and indicate whether the wave group will focus or not: the red color marks wave groups predicted to evolve into a rogue wave. Orange, yellow, and green colors indicate wave groups with predicted amplitudes that have descending order and are below the rogue-wave threshold.

the corresponding prediction scheme are shown in Fig. 4. The blue lines indicate experimental measurements. Wave groups with predicted wave amplitude that exceeds the rogue-wave threshold (twice the significant wave height) are noted with red color. Orange, yellow, and green colors indicate wave groups with predicted amplitudes that have descending order and are below the rogue-wave threshold.

First, we can clearly notice the focusing of the initially small in amplitude Peregrine wave packets to extreme waves. On the left-hand side of Fig. 4 the maximal wave height is 0.054 m and indeed exceeds twice the significant wave height, satisfying the formal definition of ocean rogue waves, whereas in the case depicted on the right-hand side, which shows a case of spontaneous focusing in the wave train, the maximal wave measured is 0.045 m and as such, this abnormality index of 1.8 is slightly below the latter threshold criteria. Here, we emphasize that the oceanographic definition of rogue waves is based on an *ad hoc* approach [3]. Indeed, for large waves having heights that correspond to 1.5 times the significant wave height could be as dangerous as well.

Note that due to discrete positioning of the wave gauges along the flume, it may be possible that higher amplitude waves have not been captured in the spacing between two wave gauges. Nevertheless, the prediction scheme was clearly successful in detecting the embedded pulsating Peregrine wave packet; see each of the red time windows in Fig. 4, proving the applicability of the method to detect wave groups undergoing modulation instability in unidirectional seas. Note that the water wave dynamics in the wave flume is much more complex than described by the NLS and MNLS. In fact, breaking and higher-order nonlinear interactions are inevitable features. The success of the scheme in identifying the unstable wave packets at early stages of focusing proves, however, that the main dynamics can be indeed described by means of weakly nonlinear evolution equations.

For reference we have included a prediction based on second-order theory, see Fig. 5. A second-order expansion of the sea surface can capture the effects of wave steepness, with no approximations other than the truncation of the expansion

at the second order, i.e., maintaining quadratic nonlinearities of the amplitudes in (5). For the case of the wave group that evolves into a rogue wave, shown in Fig. 4 (left), we utilize the measurement at $x = 0$ and predict the wave height at the following measurement stations using second-order theory [60]. The height of the Peregrine at $x = 5$ is indicated by the dashed line. The second-order theory is not able to predict the near doubling of the surface elevation that we see in the experimental measurements of the embedded Peregrine breather dynamics. This is expected, taking into account the important energy transfers between harmonics due to the severe focusing involved in the Peregrine breather-type rogue wave, which cannot be captured by the second-order theory.
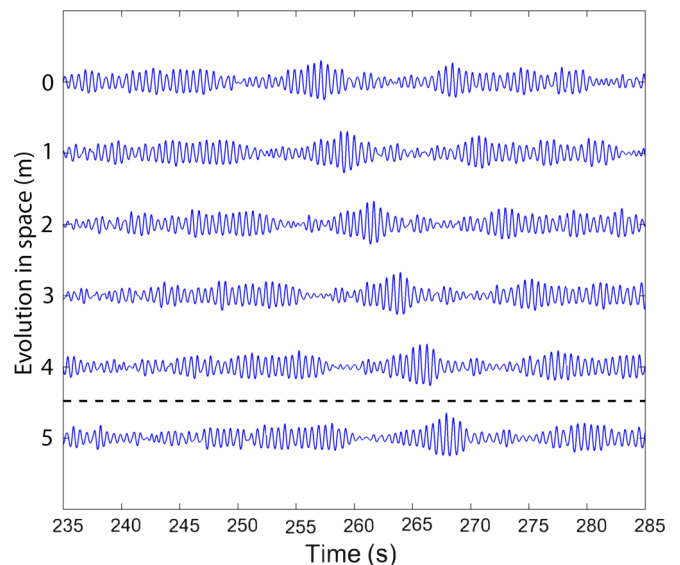

FIG. 5. Prediction of wave evolution based on second-order theory for the rogue wave presented in Fig. 4(a). The experimentally measured height of the embedded Peregrine at $x = 5$ is indicated by the dashed line. As expected, second-order theory is not able to capture the observed near doubling of the surface elevation.
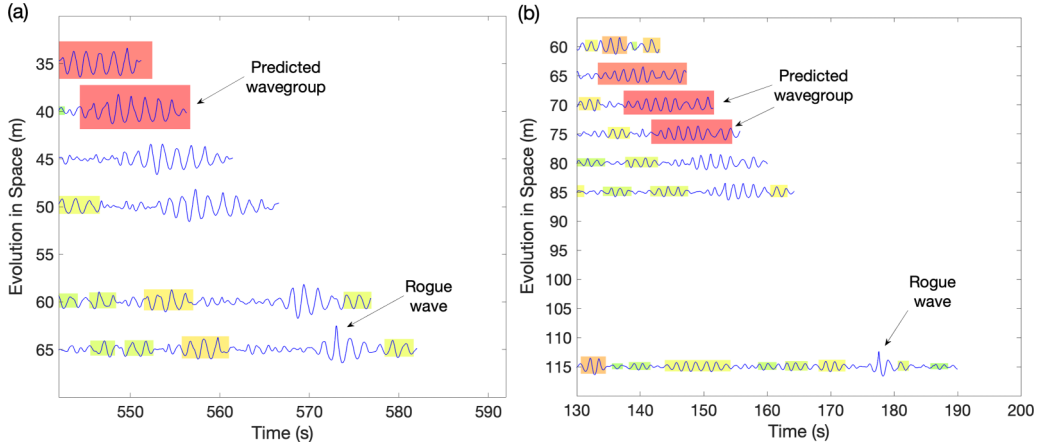
FIG. 6. Successful prediction of a rogue wave occurring in an irregular wave field characterized by a JONSWAP spectrum with $\gamma = 3.3$ (a) and $\gamma = 6$ (b). The blue curves indicate the experimental measurements. The colored boxes show the prediction and indicate whether the wave group will focus or not: red marks wave groups predicted to evolve into a rogue wave; orange, yellow, and green colors indicate wave groups with predicted amplitudes that have descending order and are below the rogue-wave threshold.

B. Spontaneous emergence of rogue waves from a JONSWAP spectrum

A time series built from a JONSWAP spectrum is characterized by many wave packets whose amplitudes and widths depend on the total power of the spectrum and on its width, respectively. It has been established that if the spectrum is narrow, the wave packets will have larger correlation lengths and, if they are sufficiently large in amplitude, they can go through a modulation instability process [58] which eventually culminates in a rogue wave. Similarly, with the previous section, the goal here is to establish *a priori* which of the initial packets will eventually go through this process.

1. Description of the experiments

The data we use here have been collected during an experimental campaign performed at Marintek in Trondheim (Norway) in one of the longest existing water wave flumes. The results of the experiments are collected in the following papers [48,61–63]. Here, we report only the main features of the experimental setup: the length of the flume is 270 m and its width is 10.5 m. The depth of the tank is 10 m for the first 85 m, then 5 m for the rest of the flume. We have employed waves of 1.5 s of peak period; this implies that with some good approximations waves can be considered as propagating in infinite water depth, regardless of the mentioned bathymetry variation. A flap-type wave maker and a sloping beach are located at the beginning and at the far end of the tank so that wave reflection is minimized. The wave surface elevation was measured simultaneously by 19 probes placed at different

locations along the flume; conductance wave gauges were used.

The data here presented consist of three different experiments with different values of the parameters in the JONSWAP spectrum. More specifically, we choose $f_p = 0.667$ Hz for all experiments and $\gamma = 1$ and $H_s = 0.11$ m for the first one, $\gamma = 3.3$ and $H_s = 0.14$ m for the second one, and $\gamma = 6$ and $H_s = 0.16$ m for the last one (see [48] for details).

2. Assessment of the scheme for different parameters

In Fig. 6 we present two cases of successful prediction. The blue curves indicate the experimental measurements. The colored boxes indicate whether the wave group will focus or not. Specifically, wave groups marked with red color will undergo modulation instability and will lead to a rogue wave. Orange, yellow, and green colors indicate wave groups with predicted amplitudes that have descending order and are below the rogue-wave threshold. The moment we have measured through the first probe the elevation of the wave group we are able to predict how the height of the wave group will evolve and whether it will exceed the rogue-wave threshold. This prediction is done by using the described algorithm in Sec. 2.2. The prediction is confirmed by measurements through a probe that is placed further in the wave tank. In Table I we summarize the statistics for the prediction scheme. We observe that in all cases of γ the prediction is accurate while we miss very few rogue waves. The prediction time, i.e., the duration from when we first predict a particular rogue wave to the time when it is first detected, has $\mathcal{O}(10T_p)$ length. This is consistent with the numerical studies in [15,36].

TABLE I. Prediction statistics for rogue waves occurring in a JONSWAP spectrum with different parameters. Prediction time is nondimensionalized by the peak wave period, T_p.

Parameter γ	Correct	False-negative	False-positive	Prediction time (T_p)
$\gamma = 1$	80% (17/19)	10% (2/19)	34% (9)	14.9
$\gamma = 3.3$	100% (42/42)	0% (0/42)	40% (28)	17.3
$\gamma = 6$	95% (58/61)	5% (3/61)	34% (30)	15.3
All cases	96% (117/122)	5% (5/122)	36% (67)	16

Despite the good behavior of the algorithm in terms of not missing extreme events, it has a relatively large false-positive rate. We attribute this characteristic to the existence of noise or other imperfections of wave profiles that are a result of wave breaking, for instance, which is inevitable in this experimental setup and thus may lead to overestimation of the height of the wave group. Moreover, it is possible that the actual false-positive rate is lower than 36%, since we have measurements of the wave field only at the location of the probes, while a wave group may exceed the extreme height threshold only at a location where we have not been monitoring along the wave flume. Subsequently, this would then be classified as a false-positive.

Additionally, even if the wave dynamics were governed exactly by MNLS, the false-positive rate would not be 0%. We studied this problem in [36] and observed a false-positive rate of 20%–25%. Part of the reason that the false-positive rate is relatively high is due to the binary nature of these predictions. For example, if we predict that a rogue wave will occur and a wave with height equal to 99% of the rogue-wave threshold occurs, then this prediction is recorded as a false-positive.

IV. CONCLUSIONS

To summarize, we have applied a reduced-order predictive scheme for extreme events caused by spatially localized modulation instability, based on the dynamics of MNLS, to two types of laboratory data: in the first the extreme events have been modeled to arise from seeded unstable deterministic breather dynamics embedded in a JONSWAP sea state, while in the second the extreme events have emerged spontaneously from the JONSWAP wave field. This provides evidence that our reduced-order predictive scheme, previously considered only in the context of numerical simulations, can perform well even in experimental settings where the assumed physical model does not apply exactly and the wave field measurements contain noise.

Considering the fact that during the laboratory experiments the wave profiles were measured discretely along the flume, some of the false-positive predictions may still be regarded as *successful*. Nevertheless, the experimental wave fields considered here are simpler than typical wave fields on the open ocean, and further studies are required to assess applicability of this scheme to directional seas [37]. Indeed, unidirectional wave propagation can be related only to swell propagation, whereas sea dynamics can be more complex in nature. Spatial measuring techniques using a stereo camera are promising in capturing water surface distributions [64,65].

Additionally, applications to other nonlinear dispersive media are inevitable. Indeed, it is well known that the unidirectional wave propagation in Kerr media follows NLS-type evolution equations with better accuracy than in the case of water waves. Since the degree of nonlinearity of electromagnetic waves propagating in nonlinear fiber optics can be accurately controlled by the Kerr medium [66,67], breaking thresholds are much higher [68] compared to water waves, so a better accuracy of the scheme is expected.

[1] P. Müller, C. Garrett, and A. Osborne, Rogue waves, Oceanography **18**, 66 (2005).

[2] K. Dysthe, H. Krogstad, and P. Muller, Oceanic rogue waves, Annu. Rev. Fluid Mech. **40**, 287 (2008).

[3] C. Kharif, E. Pelinovsky, and A. Slunyaev, *Rogue Waves in the Ocean* (Springer, New York, 2009).

[4] M. Onorato, S. Residori, U. Bortolozzo, A. Montina, and F. T. Arecchi, Rogue waves and their generating mechanisms in different physical contexts, Phys. Rep. **528**, 47 (2013).

[5] *Rogue and Shock Waves in Nonlinear Dispersive Media*, edited by M. Onorato, S. Rsidori, and F. Baronio, Lecture Notes in Physics Vol. 926 (Springer International Publishing, Cham, Switzerland, 2008).

[6] S. Haver, "A possible freak wave event measured at the Draupner jacket January 1 1995," *Rogue waves 2004*, pp. 1–8, 2004.

[7] P. C. Liu, A chronology of freauqe wave encounters, Geofizika **24**, 57 (2007).

[8] H. Bailung, S. K. Sharma, and Y. Nakamura, Observation of Peregrine Solitons in a Multicomponent Plasma with Negative Ions, Phys. Rev. Lett. **107**, 255005 (2011).

[9] F. Fontanela, A. Grolet, L. Salles, A. Chabchoub, and N. Hoffmann, Dark solitons, modulation instability and breathers in a chain of weakly nonlinear oscillators with cyclic symmetry, J. Sound Vib. **413**, 467 (2018).

[10] D. Solli, C. Ropers, P. Koonath, and B. Jalali, Optical rogue waves, Nature (London) **450**, 1054 (2007).

[11] J. M. Dudley, F. Dias, M. Erkintalo, and G. Genty, Instabilities, breathers and rogue waves in optics, Nat. Photon. **8**, 755 (2014).

[12] P. Walczak, S. Randoux, and P. Suret, Optical Rogue Waves in Integrable Turbulence, Phys. Rev. Lett. **114**, 143903 (2015).

[13] S. Annenkov and V. Shrira, On the predictability of evolution of surface gravity and gravity-capillary waves, Phys. D (Amsterdam, Neth.) **152**, 665 (2001).

[14] P. A. E. M. Janssen, Nonlinear four-wave interactions and freak waves, J. Phys. Oceanogr. **33**, 863 (2003).

[15] M.-R. Alam, Predictability horizon of oceanic rogue waves, Geophys. Res. Lett. **41**, 8477 (2014).

[16] D. G. Dommermuth and D. K. P. Yue, A high-order spectral method for the study of nonlinear gravity waves, J. Fluid Mech. **184**, 267 (1987).

[17] B. J. West, K. A. Brueckner, R. S. Janda, D. M. Milder, and R. L. Milton, A new numerical method for surface hydrodynamics, J. Geophys. Res. **92**, 11803 (1987).

[18] M. Onorato, L. Cavaleri, S. Fouques, O. Gramstad, P. Janssen, J. Monbaliu, A. Osborne, C. Pakozdi, M. Serio, C. Stansberg *et al.*, Statistical properties of mechanically generated surface gravity waves: A laboratory experiment in a three-dimensional wave basin, J. Fluid Mech. **627**, 235 (2009).

[19] A. Toffoli, O. Gramstad, K. Trulsen, J. Monbaliu, E. Bitner-Gregersen, and M. Onorato, Evolution of weakly nonlinear random directional waves: Laboratory experiments and numerical simulations, J. Fluid Mech. **664**, 313 (2010).

[20] W. Xiao, Y. Liu, G. Wu, and D. Yue, Rogue wave occurrence and dynamics by direct simulations of nonlinear wave-field evolution, J. Fluid Mech. **720**, 357 (2013).

[21] M. A. Mohamad, W. Cousins, and T. P. Sapsis, A probabilistic decomposition-synthesis method for the quantification of rare events due to internal instabilities, J. Comput. Phys. **322**, 288 (2016).

[22] M. Onorato, A. R. Osborne, and M. Serio, Extreme wave events in directional, random oceanic sea states, Phys. Fluids **14**, L25 (2002).

[23] W. Cousins and T. P. Sapsis, The unsteady evolution of localized unidirectional deep water wave groups, Phys. Rev. E **91**, 063204 (2015).

[24] T. B. Benjamin and J. E. Feir, The disintegration of wave trains on deep water, J. Fluid. Mech. **27**, 417 (1967).

[25] C. Garrett and J. Gemmrich, Rogue waves, Phys. Today **62**(6), 62 (2009).

[26] T. B. Benjamin and K. Hasselmann, Instability of periodic wavetrains in nonlinear dispersive systems [and discussion], Proc. R. Soc. London, Ser. A, **299**, 59 (1967).

[27] M. P. Tulin and T. Waseda, Laboratory observations of wave group evolution, including breaking effects, J. Fluid Mech. **378**, 197 (1999).

[28] A. Chabchoub, N. P. Hoffmann, and N. Akhmediev, Rogue Wave Observation in a Water Wave Tank, Phys. Rev. Lett. **106**, 204502 (2011).

[29] A. Chabchoub, N. Hoffmann, M. Onorato, and N. Akhmediev, Super Rogue Waves: Observation of a Higher-Order Breather in Water Waves, Phys. Rev. X **2**, 011015 (2012).

[30] V. E. Zakharov, Stability of periodic waves of finite amplitude on the surface of a deep fluid, J. Appl. Mech. Tech. Phys. **9**, 190 (1968).

[31] A. R. Osborne, M. Onorato, and M. Serio, The nonlinear dynamics of rogue waves and holes in deep-water gravity wave trains, Phys. Lett. A **275**, 386 (2000).

[32] V. E. Zakharov and L. A. Ostrovsky, Modulation instability: The beginning, Phys. D (Amsterdam, Neth.) **238**, 540 (2009).

[33] T. A. A. Adcock and P. H. Taylor, Focusing of unidirectional wave groups on deep water: An approximate nonlinear

Schrodinger equation-based model, Proc. R. Soc. London, Ser. A **465**, 3083 (2009).

[34] V. P. Ruban, Gaussian variational ansatz in the problem of anomalous sea waves: Comparison with direct numerical simulation, J. Exp. Theor. Phys. **120**, 925 (2015).

[35] W. Cousins and T. P. Sapsis, Quantification and prediction of extreme events in a one-dimensional nonlinear dispersive wave model, Phys. D (Amsterdam, Neth.) **280-281**, 48 (2014).

[36] W. Cousins and T. P. Sapsis, Reduced order precursors of rare events in unidirectional nonlinear water waves, J. Fluid Mech. **790**, 368 (2016).

[37] M. Farazmand and T. P. Sapsis, Reduced-order prediction of rogue waves in two-dimensional deep-water waves, J. Comput. Phys. **340**, 418 (2017).

[38] K. Trulsen and C. T. Stansberg, Spatial evolution of water surface waves: Numerical simulation and experiment of bichromatic waves, in *The Eleventh International Offshore and Polar Engineering Conference* (The International Society of Offshore and Polar Engineers, Stavanger, Norway, 2001), pp. 71–77.

[39] N. Akhmediev, J. M. Soto-Crespo, A. Ankiewicz, and N. Devine, Early detection of rogue waves in a chaotic wave field, Phys. Lett. A **375**, 2999 (2011).

[40] N. Akhmediev, A. Ankiewicz, J. M. Soto-Crespo, and J. M. Dudley, Rogue wave early warning through spectral measurements?, Phys. Lett. A **375**, 541 (2011).

[41] K. B. Dysthe, Note on a modification to the nonlinear Schrodinger equation for application to deep water waves, Proc. R. Soc. London, Ser. A **369**, 105 (1979).

[42] J. M. Dudley and G. Genty, Supercontinuum light, Phys. Today **66**(7), 29 (2013).

[43] K. Trulsen and K. B. Dysthe, A modified nonlinear Schrödinger equation for broader bandwidth gravity waves on deep water, Wave Motion **24**, 281 (1996).

[44] B. Kibler, Rogue breather structures in nonlinear systems with an emphasis on optical fibers as testbeds, *Shaping Light in Nonlinear Optical Fibers* (John Wiley & Sons, New Jersey, 2017), p. 293.

[45] N. Akhmediev and A. Ankiewicz, *Solitons: Nonlinear Pulses and Beams* (Chapman & Hall, London, 1997).

[46] A. Tikan, C. Billet, G. El, A. Tovbis, M. Bertola, T. Sylvestre, F. Gustave, S. Randoux, G. Genty, P. Suret *et al.*, Universality of the Peregrine Soliton in the Focusing Dynamics of the Cubic Nonlinear Schrödinger Equation, Phys. Rev. Lett. **119**, 033901 (2017).

[47] A. V. Slunyaev and V. Shrira, On the highest non-breaking wave in a group: Fully nonlinear water wave breather versus weakly nonlinear theory, J. Fluid Mech. **735**, 203 (2013).

[48] M. Onorato, A. R. Osborne, M. Serio, L. Cavaleri, C. Brandini, and C. T. Stansberg, Extreme waves, modulational instability and second order theory: Wave flume experiments on irregular waves, Eur. J. Mech. B. Fluids **25**, 586 (2006).

[49] A. Chabchoub, N. Hoffmann, M. Onorato, G. Genty, J. M. Dudley, and N. Akhmediev, Hydrodynamic Supercontinuum, Phys. Rev. Lett. **111**, 054104 (2013).

[50] A. Osborne, *Nonlinear Ocean Waves & The Inverse Scattering Transform* (Academic Press, New York, 2010), Vol. 97.

[51] A. Goullet and W. Choi, A numerical and experimental study on the nonlinear evolution of long-crested irregular waves, Phys. Fluids (1994–present) **23**, 1 (2011).

[52] D. H. Peregrine, Water waves, nonlinear Schrödinger equations and their solutions, J. Aust. Math. Soc., Ser. B, **25**, 16 (1983).

[53] A. Chabchoub, Tracking Breather Dynamics in Irregular Sea State Conditions, Phys. Rev. Lett. **117**, 144103 (2016).

[54] N. Akhmediev, V. M. Eleonskii, and N. E. Kulagin, Generation of periodic trains of picosecond pulses in an optical fiber: Exact solutions, Sov. Phys. JETP **62**, 894 (1985).

[55] J. M. Dudley, G. Genty, F. Dias, B. Kibler, and N. Akhmediev, Modulation instability, Akhmediev breathers and continuous wave supercontinuum generation, Opt. Exp. **17**, 21497 (2009).

[56] B. Kibler, J. Fatome, C. Finot, G. Millot, F. Dias, G. Genty, N. Akhmediev, and J. M. Dudley, The Peregrine soliton in nonlinear fibre optics, Nat. Phys. **6**, 790 (2010).

[57] G. J. Komen, L. Cavaleri, M. Donelan, K. Hasselmann, S. Hasselmann, and P. Janssen, *Dynamics and Modeling of Ocean Waves* (Cambridge University Press, Cambridge, UK, 1996).

[58] M. Onorato, A. R. Osborne, M. Serio, and S. Bertone, Freak Waves in Random Oceanic Sea States, Phys. Rev. Lett. **86**, 5831 (2001).

[59] A. Chabchoub and M. Fink, Time-Reversal Generation of Rogue Waves, Phys. Rev. Lett. **112**, 124101 (2014).

[60] G. Z. Forristall, Wave crest distributions: Observations and second-order theory, J. Phys. Oceanogr. **30**, 1931 (2000).

[61] M. Onorato, A. R. Osborne, M. Serio, C. Brandini, and C. T. Stansberg, Observation of strongly non-Gaussian statistics for random sea surface gravity waves in wave flume experiments, Phys. Rev. E **70**, 067302 (2004).

[62] M. Onorato, A. R. Osborne, M. Serio, and L. Cavaleri, Modulational instability and non-Gaussian statistics in experimental random water-wave trains, Phys. Fluids **17**, 078101 (2005).

[63] R. El Koussaifi, A. Tikan, A. Toffoli, S. Randoux, P. Suret, and M. Onorato, Spontaneous emergence of rogue waves in partially coherent waves: A quantitative experimental comparison between hydrodynamics and optics, Phys. Rev. E **97**, 012208 (2018).

[64] A. Benetazzo, Measurements of short water waves using stereo matched image sequences, Coastal Eng. **53**, 1013 (2006).

[65] K. Mozumi, T. Waseda, and A. Chabchoub, 3D stereo imaging of abnormal waves in a wave basin, in *ASME 2015 34th International Conference on Ocean, Offshore and Arctic Engineering* (American Society of Mechanical Engineers, New York, 2015), p. V003T02A027.

[66] P. Suret, R. Koussaifi, A. Tikan, C. Evain, S. Randoux, C. Szwaj, and S. Bielawski, Single-shot observation of optical rogue waves in integrable turbulence using time microscopy, Nat. Commun. **7**, 13136 (2016).

[67] M. Närhi, B. Wetzel, C. Billet, S. Toenger, T. Sylvestre, J.-M. Merolla, R. Morandotti, F. Dias, G. Genty, and J. M. Dudley, Real-time measurements of spontaneous breathers and rogue wave events in optical fibre modulation instability, Nat. Commun. **7**, 13675 (2016).

[68] W. Tomlinson, R. H. Stolen, and A. M. Johnson, Optical wave breaking of pulses in nonlinear optical fibers, Opt. Lett. **10**, 457 (1985).